sciendo

Bio-Algorithms and Med-Systems 2022; 18(1): 151-157

Research article

Carina Rząca*, Urszula Jankowska and Ewa Łucja Stępień

Proteomic profiling of exosomes derived from pancreatic beta-cells cultured under hyperglycemia

https://doi.org/10.2478/bioal-2022-0085
Received December 5, 2021; accepted December 11, 2022; published online December 19, 2022.

Keywords: proteomic, exosomes, hyperglycemia, mass spectrometry.

Abstract:

Introduction

Cargo carried by extracellular vesicles (EVs) is considered a promising diagnostic marker, especially proteins. EVs can be divided according to their size and way of biogenesis into exosomes (diameter < 200 nm) and ectosomes (diameter > 200 nm). Exosomes are considered to be of endocytic origin, and ectosomes are produced by budding and shedding from the plasma membrane [1].

Methods

The first step of this study was a characterization of the exosome sample. Using Tunable Resistive Pulse Sensing (qNano) size distribution and concentration were measured. The mean size of exosomes was 120±9.17 nm. In the present study, a nano liquid chromatography coupled with tandem mass spectrometry (nanoLC-MS/MS) was used to compare protein profiles of exosomes secreted by pancreatic beta cells (1.1B4) grown under normal glucose (NG, 5 mM D-glucose) and high glucose (HG, 25 mM D-glucose) conditions. The EV samples were lysed, and proteins were denatured, digested, and analyzed using a Q-Exactive mass spectrometer coupled with the UltiMate 3000 RSLC nano system. The nanoLC-MS/MS data were searched against the SwissProt *Homo sapiens* database using MaxQuant software and protein quantitation was done by the MaxLFQ algorithm. Statistical analysis was carried out with Perseus software. Further bioinformatic analysis was performed using the FunRich 3.1.4 software with the UniProt protein database and String [2].

Results

As a result of the nanoLC-MS/MS analysis more than 1,000 proteins were identified and quantified in each sample. The average number of identified proteins in exosomes was 1,397. Label-free quantitative analysis showed that exosome composition differed significantly between those isolated under NG and HG conditions. Many pathways were down-regulated in HG, particularly the ubiquitin-proteasome pathway. In addition, a significant up-regulation of the Ras-proteins pathway was observed in HG.

Conclusion

Our description of exosomes protein content and its related functions provides the first insight into the EV interactome and its role in glucose intolerance development and diabetic complications. The results also indicate the applicability of EV proteins for further investigation regarding their potential as circulating *in vivo* biomarkers.

***Corresponding author: Carina Rząca**, M. Smoluchowski Institute of Physics, Faculty of Physics, Astronomy and Applied Computer Science, Jagiellonian University, Krakow, Poland; and Centre for Theranostics, Jagiellonian University, Kraków, Poland. Email: carina.rzaca@doctoral.uj.edu.pl

Urszula Jankowska, Proteomics and Mass Spectrometry Core Facility, Malopolska Centre of Biotechnology, Jagiellonian University, Krakow, Poland

Ewa Łucja Stępień, Instytut Fizyki im. Mariana Smoluchowskiego, Uniwersytet Jagielloński, 11 Łojasiewicza St., 30-348 Kraków, Poland; Total-Body Jagiellonian-PET Laboratory, Jagiellonian University, Kraków, Poland; and Centre for Theranostics, Jagiellonian University, Kraków, Poland, Phone: +48 12 664 47 62. E-mail: e.stepien@uj.edu.pl

Introduction

In response to high blood sugar level, pancreatic β cells secrete insulin in a regulated manner to maintain glucose homeostasis. Peripheral insulin sensitivity is attenuated by increased adiposity that elevates free fatty acid levels in the circulation. Acute exposure of β-cells to elevated glucose levels causes reversible insensitivity to glucose whereas chronic exposure may either cause irreversible loss of β-cell function and apoptosis (glucotoxicity) [3, 4].

Extracellular vesicles (EVs) are actively secreted by most living cells and play a key role in paracrine and endocrine intercellular communication via the exchange

of biological molecules. The canonical classification of EV distinguishes three subpopulations: exosomes derived from endosomes (ranging in diameter from 50–150 nm), cell ectosomes (150–1,000 nm in diameter), and apoptotic bodies (1,000–5,000 nm in diameter). Secreted EVs reflect the physiology and pathology of the cell of their origin, and they have an important function in cellular homeostasis, disease pathogenesis, and diagnostics. Moreover, EVs are gaining attention in clinics as therapeutics and drug delivery vehicles, transferring bioactive molecules such as miRNAs [5–8], proteins [9, 10], genes [11], and other therapeutic agents to target cells for therapeutic purposes [12]. Recent *in vivo* and *in vitro* studies have shown that the molecular composition of EVs is changing because of hyperglycemia (HG) [13, 14], and these changes can be considered as diagnostic and prognostic biomarkers.

In our study, nano liquid chromatography coupled with tandem mass spectrometry (nanoLC-MS/MS) was used to profile and compare the protein composition of exosomes secreted by pancreatic beta cells (1.1B4) grown under normal (5 mM D-glucose) and high glucose (25 mM D-glucose) conditions.

Methods

Cell culture

The human pancreatic β-cell line (1.1B4) was maintained in RPMI1640 medium supplemented with 10% fetal bovine serum (FBS), 200 mM L-glutamine, penicillin (100 unit/mL) and streptomycin (100 µg/mL). Cells were grown in a monolayer at 37 °C and a humidified atmosphere of 5% CO2 until reaching about 80% of confluence. Half of the dishes were cultured under normal glucose (NG) conditions (5 mM D-glucose), while the second half was grown under long-term (3 passages) HG conditions (25 mM D-glucose).

Exomes isolation

Sub-confluent cells were maintained for 24 h in RPMI1640 medium without FBS. Conditioned media were collected and centrifugated at 400 × g (10 min), and 3,100 × g (25 min), the remaining cells and cellular debris were pelleted and discarded, whereas supernatant was collected for filtration. The 1,000 kDa molecular weight cut-off dialysis cellulose membranes (Spectra/Por Biotech) at low pressure (–0.3 Bar) were used to concentrate sample to 1 ml volume. In the next step, the concentrated sample was centrifuged at 7,000 × g (20 min) to remove apoptotic bodies. The supernatant was collected and ultracentrifuged at 150,000 × g (1.5h), the next pellet was suspended in 50 µL of PBS.

qNano

The size distribution and EVs concentration were determined by the Tunable Resistive Pulse Sensing (TRPS) technique (qNano; Izon, Christchurch, New Zealand). The calibration was performed using CPC200 polystyrene beads suspended in PBS. The particle number was counted using NP150 nanopore membranes stretched to 47 mm. The data were analyzed using the Izon Control Suite software (version 3.4).

nanoLC-MS/MS analysis

For proteome analysis, the exosome pellets in four replicates per group were suspended in 50 µL of lysis buffer (1% SDS, 100 mM Tris-HCl pH 7.6). Next, the samples were denatured at 95 ˚C for 5 min and sonicated with Bioruptor Pico (Diagenode, Seraing, Belgium) (5 cycles of 30s/30s on/off). Then, lysates were centrifuged at 20,000 × g for 10 min at 20 °C, and supernatants were collected. Proteins were precipitated by adding trichloroacetic acid (TCA) to the sample in a ratio of 1 to 4 and incubated overnight at –20 °C. The samples were centrifugated at 10,000× g for 15 min at 10 °C. Pellets were washed with ice-cold acetone and resuspended in 100 µL of 10 mM HEPES (pH 8.5). Next, the samples were prepared using paramagnetic bead technology based on the Single-Pot Solid-Phase-Enhanced Sample Preparation (SP3) [15]. A 1:1 ratio of GE65152105050250 and GE45152105050250 SpeedBeads™ was used. The proteins were reduced with dithiothreitol, alkylated with iodoacetamide, and digested with Trypsin/Lys-C Mix. Peptides were analyzed using an UltiMate 3000 RSLCnano System coupled with a Q-Exactive mass spectrometer (Thermo Fisher Scientific) with DPV-550 Digital PicoView nanospray source (New Objective). The sample was loaded onto a trap column (Acclaim PepMap 100 C18, 75 µm × 20 mm, 3 µm particle, 100 Å pore size) in 0.05% trifluoroacetic acid (TFA) and 2% acetonitrile at a flow rate of 5 µL/min, and further resolved on an analytical column (Acclaim PepMap RSLC C18, 75 µm × 500 mm, 2 µm particle, 100 Å pore size) with a 240 min gradient from 2% to 40% acetonitrile in 0.05% formic acid at a flow rate of 250 nL/min. The Q-Exactive was

operated in a data-dependent mode using the top twelve method. The MS and MS/MS spectra were acquired at resolutions of 70,000 and 17,500, respectively. Peptides were dynamically excluded from fragmentation within 30 s.

Bioinformatics analysis

Raw MS data files were processed using Max Quant software (version 1.6.7.0) [16]. Peak lists were searched against the forward and reverse Swissprot database (*Homo sapiens*, 20,394 sequences downloaded on February 8, 2021) using the integrated Andromeda search engine [17]. The false discovery rate (FDR) for the peptide and protein identification was set to 1%. All proteins that cannot be distinguished based on the identified peptides were merged into one protein group. Relative quantification and normalization were performed with the MaxLFQ label-free algorithm. The MaxQuant output table was further processed with the use of the Perseus platform (version 1.6.15.0) [18]. The proteins identified in the decoy database, contaminants, and proteins only identified by site were filtered out. All bioinformatic analyses were executed on LFQ intensities transformed to a logarithmic scale with base two. The student's t-test with the permutation-based FDR set to 5% was used to reveal changes in protein abundances under NG and HG conditions. The statistical analysis was performed for the proteins with a minimum of 3 valid LFQ intensity values in both groups. Proteins were considered as a differential when they were identified based on at least 2 peptides and their fold change was of at least 1.5.

Additionally, the overlap between identified proteins in exosomes and Vesiclepedia (http://www.microvesicles.org) was examined with the use of FunRich version 3.1.4 software with the UniProt database as a reference. Interactomes were prepared using String version 11.0 (https://string-db.org). Obtained data are provided in the Supplementary file [19].

Results and discussion

The purity of the exosome was evaluated with the use of the TRPS technique (qNano). The analysis of the samples by qNano (Fig. 1) confirmed that with a diameter in the range of 100–300 nm in NG and HG conditions, mean 120±9.17 nm, the isolated EVs were predominantly in range typical for exosomes.

We compared exosome proteins identified in our study to those known vesicular proteins in the Vesiclepedia databases (Fig.2). Among 13,173 proteins available in public repositories (Vesiclepedia), 44.76% of them were common with the identified proteome, including the exosomal markers: tetraspanin family members CD9, CD81, and other exosome markers, flotillin 1 (FLOT1), flotillin 2 (FLOT2) [20].

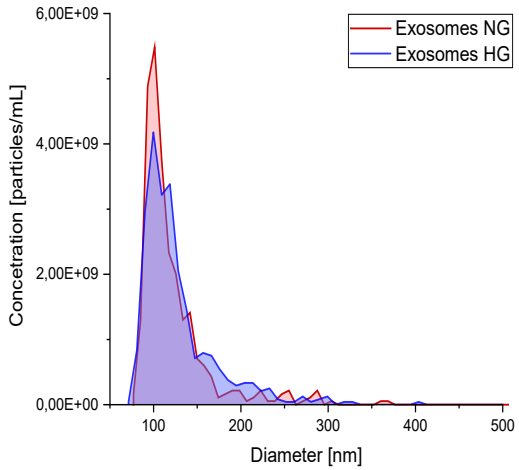

Figure 1: Size distribution and concentration of EVs isolated from pancreatic β-cells obtained by qNano system.

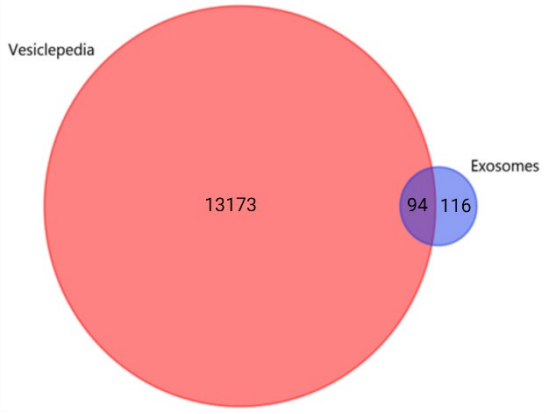

Figure 2: Venn diagram illustrating protein overlap between exosome samples with Vesiclepedia database.

Proteins are usually strongly associated with other proteins in metabolic pathways. Diagrams of functional protein association networks were prepared with the use of String. In our study, 105 proteins were up-regulated and 67 down-regulated in hyperglycemic exosomes. For up-regulated proteins, the most strongly represented pathways involved the Ras protein signal transduction, integrin-mediated signaling pathway, establishment of protein localization to the endoplasmic reticulum, and cell adhesion mediated by integrins (Fig.3A).

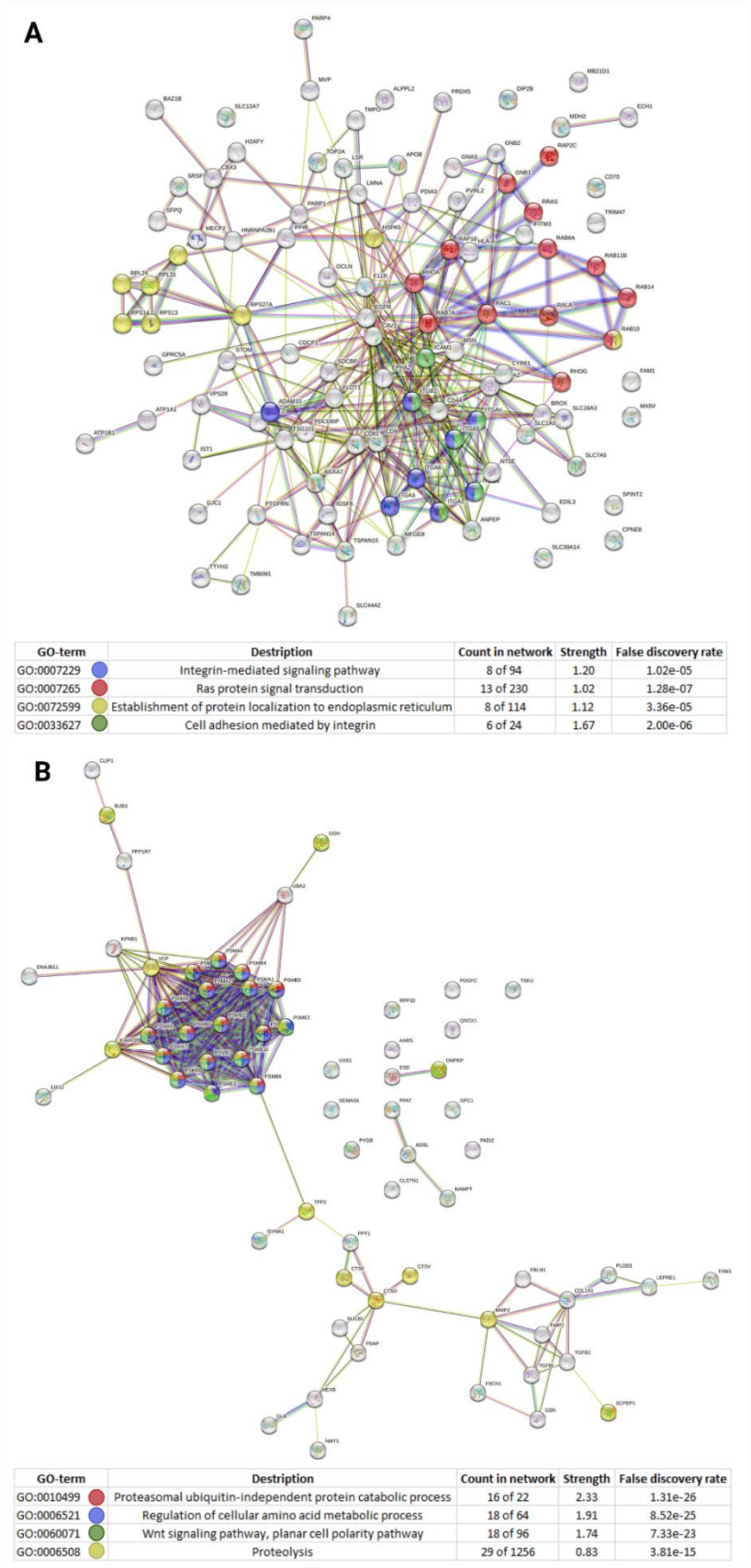

GO-term	Description	Count in network	Strength	False discovery rate
GO:0007229	Integrin-mediated signaling pathway	8 of 94	1.20	1.02e-05
GO:0007265	Ras protein signal transduction	13 of 230	1.02	1.28e-07
GO:0072599	Establishment of protein localization to endoplasmic reticulum	8 of 114	1.12	3.36e-05
GO:0033627	Cell adhesion mediated by integrin	6 of 24	1.67	2.00e-06

GO-term	Description	Count in network	Strength	False discovery rate
GO:0010499	Proteasomal ubiquitin-independent protein catabolic process	16 of 22	2.33	1.31e-26
GO:0006521	Regulation of cellular amino acid metabolic process	18 of 64	1.91	8.52e-25
GO:0060071	Wnt signaling pathway, planar cell polarity pathway	18 of 96	1.74	7.33e-23
GO:0006508	Proteolysis	29 of 1256	0.83	3.81e-15

Figure 3: Diagram of functional protein association networks prepared with the use of String database. Only strongly represented pathways are presented on the interactome. A) proteins that were up-regulated B) down-regulated in hyperglycemic exosomes.

In this study, we identified Rab6, Rab7, Rab10, Rab10, Rab11, Rab14 and Rab16 in exosomes. The small Rab GTPases consists of a family of proteins composed of approximately 70 different proteins, all belonging to the super-family of Ras GTPases [21, 22]. They canonically function as a molecular switch by cycling between GTP- and GDP-bound states. The GTP-bound form is the active form with can interact with effectors. In terms of exosome secretion, Rab GTPases plays a crucial role in intracellular vesicle transport including endosome recycling and MVB trafficking to lysosomes. Rab GTPase modulation of exosome secretion depends on cell type and exosomal cargo [23]. In their paper Savina A. et al. showed that Rab11 promotes the docking of MVBs to stimulate homotypic fusion, but the final fusion requires the presence of calcium ions (Ca^{2+}) [24]. Additionally, a rise in the intracellular Ca^{2+} concentration enhanced exosome secretion in Rab11 overexpressing K562 cells. These results suggest that both Rab11 and Ca^{2+} are involved in the homotypic fusion of MVBs [24]. Dickson L. found Rab6 is required for rapid, cisternal-specific, intra-Golgi cargo transport in HeLa cells [25].

In up-regulated proteins we also recognized other Small G proteins like RhoA and RhoG in this system. Rho proteins promote the reorganization of the actin cytoskeleton and regulate cell shape, attachment, and motility [26].

In their paper, Tasaka S. et al. showed that activation of the RhoA pathway can disrupt lung barrier function in ALI mice through increased permeability, stress fiber formation, actomyosin contraction, and paracellular gap formation in LPS-stimulated endothelial cells [27].

Analogously, down-regulated proteins in exosomes from HG were analyzed (Fig.3B), revealing enrichment in proteins related to the regulation of the cellular amino acid metabolic process, proteasomal ubiquitin-independent protein catabolic process, Wnt-signaling pathway, and proteolysis.

In the present study, we first found that the subunits of the proteasome are significantly depleted in exosomes derived from beta cells from HG. The proteasome is a cellular protease responsible for the selective degradation of most of the intracellular proteome. It recognizes, unfolds, and cleaves proteins that are destined for removal, usually by prior attachment to polymers of ubiquitin [28]. Proteasomes are composed of two related types of subunits, proteasome subunit alpha (PSMA) and proteasome subunit beta (PSMB). Alfa subunits, which form the outer two heptameric rings and are distinguished by highly conserved N-terminal extensions, and Beta subunits, which form the inner pair of heptameric rings and include the proteolytic active sites [29, 30].

In this study we identified different types of proteasome subunits alpha: PSMA1, PSMA2, PSMA3, PSMA4, PSMA5, PSMA7 and PSMB4, PSMB7, PSMB8, PSMB9, PSMB10 [31]. These subunits (PSMA1, PSMA3, PSMA4, PSMA5, PSMA6, PSMB1, PSMB6, and PSMA7) belong to the 26S proteasome complex, which is a component of the ubiquitin proteasome system (UPS), the principal proteolytic system responsible for the functional modification and the degradation of cellular proteins [32, 33].

PSMA and PSMB proteins are also part of the Wnt pathway, which regulates cell proliferation, planer cell polarity, and survival by modulating the expression of genes that control cell differentiation [34]. Kim H. showed that exosomes derived from tumor-associated macrophages enhance tumor invasion by delivering wnt5a in macrophages to breast cancer cells. Delivered wnt5a enhances tumor invasion by leading to the activation of β-catenin-independent Wnt signaling [34].

Conclusion

Our description of exosome protein content and related functions provides the first insight into the EVs interactome and its role in hyperglycemia development and diabetic complications. However, there is limited evidence in the literature to verify this statement for the exosomal protein content. Here, proteomic evaluation combined with pathway enrichment analysis is used to demonstrate that exosome protein loading reflects hyperglycemia-induced cellular changes. The results also indicate the applicability of EV proteins for further investigation regarding their potential as circulating *in vivo* biomarkers in liquid biopsy.

Research funding

This study was funded by the Polish National Science Center in the 17th edition of OPUS Competition [2019/33/B/NZ3/01004] to E. Stępień as well as the SciMat and qLife Priority Research Areas budget under the program Excellence Initiative—Research University at the Jagiellonian University [U1U/P05/NO/03.40] and Jagiellonian University flagship project.

Author contributions

All authors have accepted responsibility for the entire content of this manuscript and approved its submission.

Competing interests

Authors state no conflict of interest.

Informed consent

Not applicable.

Ethical approval

Not applicable.

References

[1] Sekuła M, Janawa G, Stankiewicz E, Stepień E. Endothelial microparticle formation in moderate concentrations of homocysteine and methionine *in vitro*. Cell Mol Biol Lett 2011;16(1):69-78.

[2] Surman M, Kędracka-Krok S, Hoja-Łukowicz D, Jankowska U, Drożdż A, Stępień E, et al. Mass spectrometry-based proteomic characterization of cutaneous melanoma ectosomes reveals the presence of cancer-related molecules. Int J Mol Sci 2020;21(8): 2934.

[3] Sharp-Tawfik A, Fletcher JD, Guergues J, Marelia-Bennett C, Wolf TJ, Coiner AM, et al. Proteomic examination of Cornus officinalis stimulated 1.1B4 human pancreatic cells reveals activation of autophagy and Keap1/Nrf2 pathway. Mol Cell Endocrinol 2022;557:111773.

[4] Vasu S, McClenaghan NH, McCluskey JT, Flatt PR. Cellular responses of novel human pancreatic β-cell line, 1.1B4 to hyperglycemia. Islets 2013;5:4,170-177.

[5] Michael A, Bajracharya SD, Yuen PST, Zhou H, Star RA, Illei GG, et al. Exosomes from human saliva as a source of microRNA biomarkers. Oral Dis 2010;16(1):34–8.

[6] Alexandru N, Badila E, Weiss E, Cochior D, Stępień E, Georgescu A. Vascular complications in diabetes: Microparticles and microparticle associated microRNAs as active players Dedicated to the 150th anniversary of the Romanian Academy. Biochem Biophys Res Commun 2016;472(1):1-10.

[7] Stępien E, Durak-Kozica M, Kamińska A, Targosz-Korecka M, Libera M, Tylko G, et al. Circulating ectosomes: Determination of angiogenic microRNAs in type 2 diabetes. Theranostics 2018; 8(14):3874-3890.

[8] Stępień E, Costa MC, Enguita FJ. miRNAtools: Advanced training using the miRNA web of knowledge. Noncoding RNA 2018;4(1):1-8.

[9] Surman M, Stępień E, Przybyło M. Melanoma-derived extracellular vesicles: Focus on their proteome. Proteomes 2019;7(2):21.

[10] Surman M, Kędracka-Krok S, Wilczak M, Rybczyński P, Jankowska U, Przybyło M. Comparative Proteomic Profiling of Ectosomes Derived from Thyroid Carcinoma and Normal Thyroid cells Uncovers Multiple Proteins with Functional Implications in Cancer. Cells. 2022 Apr 1;11(7):1184.

[11] Tran F, Boedicker JQ. Genetic cargo and bacterial species set the rate of vesicle-mediated horizontal gene transfer. Sci Rep 2017;7, 8813.

[12] Stępień E, Rząca C, Moskal P. Novel biomarker and drug delivery systems for theranostics - Extracellular vesicles. Bio-Algorithms and Med-Syst 2021;17(4):301–309.

[13] Marzec ME, Rząca C, Moskal P, Stępień EŁ. Study of the influence of hyperglycemia on the abundance of amino acids, fatty acids, and selected lipids in extracellular vesicles using TOF-SIMS. Biochem Biophys Res Commun 2022;622:30–6.

[14] Kamińska A, Roman M, Wróbel A, Gala-Błądzińska A, Małecki MT, Paluszkiewicz C, et al. Raman spectroscopy of urinary extracellular vesicles to stratify patients with chronic kidney disease in type 2 diabetes. Nanomedicine: NBM 2022;39:102468.

[15] Hughes CS, Foehr S, Garfield DA, Furlong EE, Steinmetz LM, Krijgsveld J. Ultrasensitive proteome

analysis using paramagnetic bead technology. Mol Syst Biol 2014;10(10):757.

[16] Tyanova S, Temu T, Cox J. The MaxQuant computational platform for mass spectrometry-based shotgun proteomics. Nat Protoc 2016;11,2301–2319.

[17] Cox J, Neuhauser N, Michalski A, Scheltema RA, Olsen JV, Mann M. Andromeda: A Peptide Search Engine Integrated into the MaxQuant Environment. J. Proteome Res. 2011;10(4):1794–1805.

[18] Tyanova S, Temu T, Sinitcyn P, Carlson A, Hein MY, Geiger T, et al. The Perseus computational platform for comprehensive analysis of (prote)omics data. Nat Methods 2016;13,731–740.

[19] Stępień E, Rząca C, Jankowska U. Proteomic profiling of exosomes derived from pancreatic beta-cells cultured under hyperglycemia." Kraków : Repozytorium Uniwersytetu Jagiellońskiego. 2022. doi: 10.26106/93z7-4545.

[20] Ding XQ, Wang ZY, Xia D, Wang RX, Pan XR, Tong JH. Proteomic Profiling of Serum Exosomes From Patients With Metastatic Gastric Cancer. Front Oncol 2020;10:1113.

[21] Zerial M, McBride H. Rab proteins as membrane organizers. Nat Rev Mol Cell Biol 2001;2(2):107–17.

[22] Hutagalung AH, Novick PJ. Role of Rab GTPases in membrane traffic and cell physiology. Physiol Rev 2011;91(1):119–49.

[23] Sexton RE, Mpilla G, Kim S, Philip PA, Azmi AS. Ras and exosome signaling. Semin Cancer Biol 2019;54:131–7.

[24] Savina A, Fader CM, Damiani MT, Colombo MI. Rab11 Promotes Docking and Fusion of Multivesicular Bodies in a Calcium-Dependent Manner. Traffic 2005;6(2):131–43.

[25] Dickson LJ, Liu S, Storrie B. Rab6 is required for rapid, cisternal-specific, intra-Golgi cargo transport. Sci Rep 2020;10(1):16604.

[26] McKerracher L, Ferraro GB, Fournier AE. Rho Signaling and Axon Regeneration. Int Rev Neurobiol. 2012;105:117–40.

[27] Tasaka S, Koh H, Yamada W, Shimizu M, Ogawa Y, Hasegawa N, et al. Attenuation of Endotoxin-Induced Acute Lung Injury by the Rho-Associated Kinase Inhibitor, Y-27632. Am J Respir Cell Mol Biol. 2005 Jun;32(6):504-10.

[28] Thibaudeau TA, Smith DM. A Practical Review of Proteasome Pharmacology. Pharmacol Rev 2019;71(2):170–97.

[29] Kunjappu MJ, Hochstrasser M. Assembly of the 20S proteasome. Biochimica et Biophysica Acta (BBA) - Molecular Cell Research 2014;1843(1):2–12.

[30] Bard JAM, Goodall EA, Greene ER, Jonsson E, Dong KC, Martin A. Structure and Function of the 26S Proteasome. Annu Rev Biochem 2018; 87:697.

[31] The UniProt Consortium, UniProt: the universal protein knowledgebase in 2021, Nucleic Acids Research 2021;49;D1,D480–D489.

[32] Radhakrishnan SK, Lee CS, Young P, Beskow A, Chan JY, Deshaies RJ. Transcription Factor Nrf1 Mediates the Proteasome Recovery Pathway after Proteasome Inhibition in Mammalian Cells. Mol Cell 2010;38(1):17–28.

[33] Durak-Kozica M, Paszek E, Stępień E. Role of the Wnt signalling pathway in the development of endothelial disorders in response to hyperglycaemia. Expert Rev Mol Med 2019;2:e7.

[34] Kim H, Kim DW, Cho JY. Exploring the key communicator role of exosomes in cancer microenvironment through proteomics. Proteome Sci 2019;17(1):1–14.